



HAL
open science

Estimation of spinal joint centers from external back profile and anatomical landmarks

Agathe Nerot, Wafa Skalli, Xuguang Wang

► **To cite this version:**

Agathe Nerot, Wafa Skalli, Xuguang Wang. Estimation of spinal joint centers from external back profile and anatomical landmarks. *Journal of Biomechanics*, 2018, 70, pp.96-101. 10.1016/j.jbiomech.2017.11.013 . hal-01737338

HAL Id: hal-01737338

<https://hal.science/hal-01737338>

Submitted on 19 Mar 2018

HAL is a multi-disciplinary open access archive for the deposit and dissemination of scientific research documents, whether they are published or not. The documents may come from teaching and research institutions in France or abroad, or from public or private research centers.

L'archive ouverte pluridisciplinaire **HAL**, est destinée au dépôt et à la diffusion de documents scientifiques de niveau recherche, publiés ou non, émanant des établissements d'enseignement et de recherche français ou étrangers, des laboratoires publics ou privés.

Estimation of spinal joint centers from external back profile and anatomical landmarks

A. NEROT^{†‡}, W. SKALLI[‡], X. WANG[†]

[†] *Univ Lyon, Université Claude Bernard Lyon 1, IFSTTAR, UMR_T9406, LBMC, F69622, Lyon, France*

[‡] *Institut de Biomécanique Humaine Georges Charpak, Arts et Métiers ParisTech, 75013 Paris, France*

Invited Papers-Berlin Workshop

Keywords: Joint centers prediction, External inputs, Biplanar X-rays, 3D reconstruction, Subject-specific human model

Corresponding author:

Agathe Nérot

Institut de Biomécanique Humaine Georges Charpak

151 boulevard de l'hôpital, 75013 Paris

Email: agathe.nerot@ensam.eu

Phone: +33 01 44 24 61 41

Words count: 1992

Introduction: 468

Material and methods: 761

Results: 228

Discussion: 535

Abstract

1 Defining a subject-specific model of the human body is required for motion analysis in many fields,
2 such as in ergonomics and clinical applications. However, locating internal joint centers from external
3 characteristics of the body still remains a challenging issue, in particular for the spine. Current methods
4 mostly require a set of rarely accessible (3D back or trunk surface) or operator dependent inputs (large
5 number of palpated landmarks and landmarks-based anthropometrics). Therefore, there is a need to
6 provide an alternative way to estimate joint centers only using a limited number of easily palpable
7 landmarks and the external back profile. Two methods were proposed to predict the spinal joint
8 centers: one only using 6 anatomical landmarks (ALs) (2 PSIS, T8, C7, IJ and PX) and one using both 6
9 ALs and the external back profile. Regressions were established using the X-ray based 3D
10 reconstructions of 80 subjects and evaluated on 13 additional subjects of variable anthropometry. The
11 predicted location of joint centers showed an average error 9.7 mm (± 5.0) in the sagittal plane for all
12 joints when using the external back profile. Similar results were obtained without using external back
13 profile, 9.5 mm (± 5.0). Compared to other existing methods, the proposed methods offered a more
14 accurate prediction with smaller number of palpated points. Methods have to be developed for
15 considering other postures than standing such as seated one.

16

17 Introduction

18 Accurate estimation of intervertebral joint centers is of primary importance to precisely define the
19 kinematic chain of subject-specific models for posture and motion analysis. However, few solutions
20 have been proposed to predict joint centers using easily measurable external characteristics as inputs.
21 The geometric model in Snyder *et al.* 1972 has been widely used (Kennedy 1982, Choi *et al.* 2007, Reed
22 *et al.* 1999). It provides twelve regression equations for the norm and direction of the vectors joining
23 skin markers, located on six palpated spinous processes, to six spinal joint centers. However
24 regressions were developed from only 19 male subjects' radiographic data of bones and surface
25 markers and, to our knowledge, no validation has been published yet. Other studies proposed
26 prediction equations using additional measurements such as anthropometric dimensions (body height
27 and weight), L4 skinfold and difference of L1-S1 skin distraction during maximal forward bending (Lee
28 *et al.* 1995, Chiou *et al.* 1996) in addition to palpated landmarks. However skinfold measurements
29 might show high inter-operator variability (Klipstein-Grobusch *et al.* 1997, Wang *et al.* 2000) and
30 accuracy might depend on skin thickness and skinfold compressibility (Himes *et al.*, 1979). Palpation-
31 based methods are also subject to inter-operator variation (Harlick *et al.* 2007) and could be time
32 consuming if there are a high number of points to be palpated. Therefore ideally, the prediction

33 method should require only a small number of easily palpated bony landmarks. Bryant *et al.* 1988
34 proposed an original geometric method aiming at predicting the distance between the internal spine
35 curvature and the external back profile while using only two palpated landmarks (T1 and L5) as inputs.
36 The curvilinear abscises of joint centers were estimated along the internal spinal profile. But the
37 proposed method could not fully locate the spine in the sagittal plane. Moreover, only a small sample
38 of 13 subjects from 13 to 17 years was used.

39 Recently a PCA-based method was proposed to predict internal pelvic landmarks and spine joint
40 centers location using trunk 3D surface (Nérot *et al.* 2016). The study was based on a database of 3D
41 reconstructions of bones and envelopes from low dose biplanar radiographs (Dubousset *et al.* 2010).
42 The main advantage is that the proposed method requires almost no palpation. However, the full trunk
43 skin surface is needed. A scanning device is not always a standard lab equipment. Furthermore, the
44 whole trunk surface may not easily be scanned due to the obstruction by environmental objects for
45 some applications, for example a seated person in a seat.

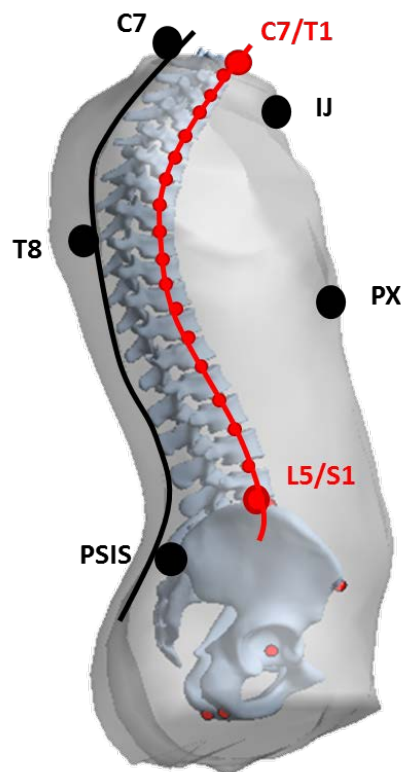
46 Using the existing database of 3D reconstructions of both internal skeleton and external body shape
47 used in Nérot *et al.* (2016), the objective of this study was to propose alternative methods for the
48 prediction of intervertebral joint centers without using the full trunk surface scan but only a small
49 amount of easily accessible input data.

50 **Material and Methods**

51 **Data**

52 With the approbation of the Ethics committee (CPP 06036) and signature of informed consents,
53 biplane radiographs of 93 subjects were collected with a low dose EOS system (EOS Imaging, France)
54 (46 females/47 males, age: [18, 76 years], height: [1.52, 1.97m], weight: [45, 103kg]). Participants were
55 asked to adopt a free standing position (Steffen *et al.* 2010). These subjects were divided into two
56 groups, a group of 80 persons for the development of the predictive methods (40 females/40 males,
57 height: [1.52, 1.88m], weight: [48, 103kg]), and a second group of 13 subjects of variable
58 anthropometry for their validation (6 females/7 males, height: [1.53, 1.97 m], weight: [45, 102kg]).
59 From these two views, 3D reconstruction of the lowers limbs, pelvis, spine and the external body
60 envelope were performed (Nérot *et al.* 2015). Subject-specific 3D reconstructions were based on the
61 deformation of parameterized and regionalized generic models on radiographic contours, allowing us
62 to isolate the thoracic region (Figure 1) and to automatically extract following internal and external
63 parameters.

- 64
- Internal parameters: Coordinates of 18 joint centers from C7/T1 to L5/S1, calculated as the
- 65 middle points of the segments joining the barycenters of the two adjacent vertebrae end-
- 66 plates (Humbert et al. 2009). Internal spine profile was approximated by a cubic spline passing
- 67 through the joint centers from C7/T1 to L5/S1.
- External parameters: anatomical landmarks (ALs) on the skin surface by virtual palpation
- 68 including posterior (PSIS) superior iliac spines, incisura jugularis (XJ), xiphoid process (XP) and
- 69 spinous processes. Bony landmarks were extracted from the parametrized subject-specific
- 70 bones models and their closest points on the envelope reconstruction were considered as an
- 71 estimation of the regular palpated landmarks. The external back curvature (or back profile)
- 72 was also approximated by a cubic spline passing through the spinous processes from C7 to L5
- 73 and limited at the PSIS midpoint.
- 74
- 75



76

77 **Figure 1.** Definition of external back (black) and internal spinal (red) profiles which are both

78 approximated by a cubic spline passing through external spinal processes and internal joint centers

79 respectively. 6 palpable AL (two PSIS, T8, C7, IJ, PX) required for the methods proposed in the

80 present study are also illustrated.

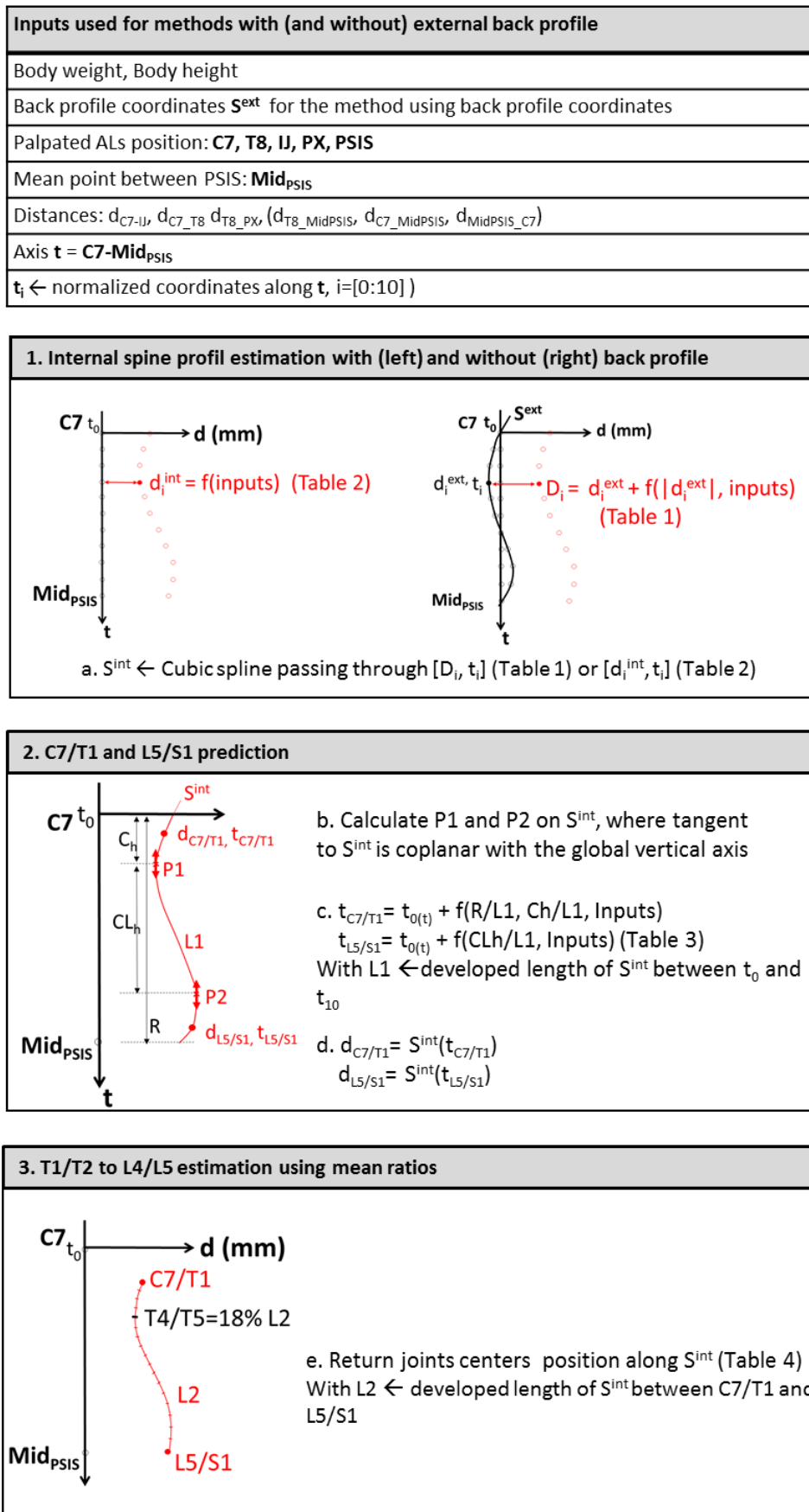
81

82

83 **Proposed predictive methods**

84 The predictive methods proposed in the present study were similar to that of Bryant *et al.* 1988 (Figure
85 2): first the internal spinal profile is predicted in a spine local coordinate system; secondly the two
86 extreme joint centers C7/T1 and L5/S1 need to be predicted; lastly the position of all other joint centers
87 can be located if their curvilinear coordinates are known.

88 The spine local coordinate system (LCS) (\mathbf{t}_0 , \mathbf{d} , \mathbf{t}) in the sagittal plane was defined with the origin \mathbf{t}_0 at
89 C7 palpated spinous process, \mathbf{t} the axis directing from C7 to the midpoint between the two palpated
90 PSIS (Figure 2.1). \mathbf{d} was the perpendicular axis to \mathbf{t} and directed forward. The internal and external
91 spinal profiles were characterized by their local coordinated $[d_i^{\text{int}}, t_i]$ and $[d_i^{\text{ext}}, t_i]$ for t_i . The coordinates
92 along \mathbf{t} were normalized by the distance between PSIS and C7 in order to compare individuals of
93 different corpulence.



94

95 **Figure 2. Successive steps for computing joint centers position using the two prediction methods**

96 Using the existing database, the regression equations were obtained for all variables required for
97 predicting the internal spinal profile, two extreme joint centers C7/T1 and L5/S1 and curvilinear
98 coordinates of other joint centers. Two methods for predicting internal spinal profile were proposed,
99 one based on the distance d_i^{int} from the t axis, one on the distance $D_i (=d_i^{int} - l_i^{ext})$ from the external
100 back profile (Figure 2.1).

101 For the internal spine profile, best predictors were searched among anthropometric dimensions (e.g.
102 stature, weight, waist circumference etc.) and distances between ALs. Pearson tests were conducted
103 to find the most correlated variables with D_i or d_i^{int} . For instance, based on *a priori* assumption, thoracic
104 depth related measurements, such as body weight, C7-IJ distance, T8-PX distance, were considered as
105 candidate predictors. Thoracic length related parameters such as T8 to PSIS, C7 to T8 distances etc.
106 were also considered in the Pearson test (Drerup et al. 2014). A stepwise regression method was
107 performed on different combinations of 2 to 6 candidates to find the most powerful combination of
108 predictors. Using the same statistical method, the t coordinates of C7/T1 and L5/S1 along the 2D spinal
109 profile were supposed to be dependent on spine curvature descriptors (Figure 2.2). Finally, the mean
110 curvilinear coordinates of joint centers were calculated to estimate the relative position of joint
111 centers along the internal spine estimate (Figure 2.3).

112

113 **Evaluation**

114 Root mean square errors (RMSE) were calculated between estimated (regression) and reference (EOS
115 based reconstructions) joint centers coordinates in the sagittal plane to assess the two proposed
116 predictive methods. First, the data from 80 subjects, from which the regression equations were
117 obtained, were used. Then an additional sample of 13 subjects was also considered for validation.

118

119 **Results**

120 **Internal spine profile prediction**

121 Up to eleven equal-distanced points along C7 to PSIS axis (t axis, Figure 2.1), with $t=[0, 0.1, \dots, 1]$, were
122 used to characterize both external and internal spine profiles. Tables 1 and 2 provide the predictors
123 for d_i^{int} and D_i . The distance D_i from the external back profile showed smaller RMS errors than the
124 distance d_i^{int} from the t axis.

125

126

127 **Table 1. Regression equations (and associated RMSE errors and coefficients of determination) of**
 128 **the distances from the external back to internal spinal profiles (D_i) for the 11 equal distanced**
 129 **points along the along the t axis. We recommend using points for $i=[0,1,2,5,6,8,9,10]$ with smaller**
 130 **RMSE.**

D_i	Regression equations	RMSE (mm)	R^2_{adj}
D_0	$0.19*d_{C7-T8} + 0.28*d_{C7-IJ} + 0.30*d_{0.6}^{ext} - 10.18$	4.8	0.7
$D_{0.1}$	$0.48*d_{C7-IJ} + 0.86*d_{0.1}^{ext} - 6.00$	4.9	0.8
$D_{0.2}$	$0.40*d_{C7-IJ} + 0.23*BW + 0.98*d_{0.2}^{ext} - 0.53*d_{0.4}^{ext} - 11.29$	5.7	0.6
$D_{0.3}$	$0.47*d_{C7-IJ} + 1.17*d_{0.3}^{ext} - 0.94*d_{0.4}^{ext} - 4.20$	6.6	0.4
$D_{0.4}$	$0.52*BW + 34.34$	6.7	0.6
$D_{0.5}$	$0.15*d_{T8-PX} + 0.34*BW + 20.45$	6.4	0.6
$D_{0.6}$	$0.17*d_{T8-PX} + 0.45*BW + 14.70$	6.5	0.6
$D_{0.7}$	$0.15*d_{T8-PX} + 0.63*BW + 12.00$	7.0	0.7
$D_{0.8}$	$0.12*d_{T8-PX} + 0.69*BW + 19.40$	6.1	0.7
$D_{0.9}$	$0.74*BW + 44.40$	6.9	0.6
D_1	$0.68*BW + 44.19$	9.3	0.4

Note: d_{C7-IJ} : C7 to IJ distance, d_i^{ext} : distance of the back profile from the $C7^{ext}$ to $PSIS^{ext}$ axis at t_i , d_{T8-PX} : T8 to PX distance, d_{C7-T8} : C7 to T8 distance, body weight in Kg.

131

132 **Table 2. Regression equations (and associated RMSE errors and coefficients of determination) of**
 133 **the distances from the $C7^{ext}$ to $PSIS^{ext}$ axis to the internal spinal profiles for the 11 equal distanced**
 134 **points along the along $C7^{ext}$ to $PSIS^{ext}$ axis. $d_{0.3}^{int}$ is not indicated as no external predictor for $d_{0.3}^{int}$**
 135 **was found by the Pearson test (mean value: 30.65 mm, RMSE, 11.6mm). We recommend using**
 136 **points for $i=[0,1,2,5,6,8,9,10]$ with smaller RMSE.**

d_i^{int}	Regression equations	RMSE (mm)	R^2_{adj}
d_0	$0.19*d_{C7-T8} + 0.24*d_{C7-IJ} + 0.13*d_{T8-PX} - 25.89$	5.3	0.7
$d_{0.1}$	$0.45*d_{C7-IJ} - 5.47$	5.0	0.5
$d_{0.2}$	$0.46*d_{C7-IJ} - 0.22*d_{T8-PX} + 0.28*BW + 3.19$	7.6	0.3
$d_{0.4}$	$-0.32*d_{T8-PX} + 0.53*BW + 63.35$	11.7	0.2
$d_{0.5}$	$-2.50*d_{C7-T8} + 2.34*d_{T8-MidPSIS} + 2.42*d_{C7-MidPSIS} + 0.36*BW + 24.96$	6.7	0.7
$d_{0.6}$	$-1.95*d_{C7-T8} - 2.07*d_{T8-MidPSIS} + 2.01*d_{C7-MidPSIS} - 0.09*d_{T8-PX} + 0.58*BW + 54.81$	6.4	0.7
$d_{0.7}$	$-1.41*d_{C7-T8} - 1.67*d_{T8-MidPSIS} + 1.52*d_{C7-MidPSIS} + 0.57*BW + 65.35$	7.3	0.6

$d_{0.8}$	$-0.81*d_{C7-T8} -1.14*d_{T8-MidPSIS} + 0.95*d_{C7-MidPSIS} + 0.70*BW + 76.41$	7.1	0.5
$d_{0.9}$	$-0.21*d_{T8-MidPSIS} + 0.84*BW + 101.58$	7.0	0.5
$d_{1.0}$	$-0.16*d_{C7-MidPSIS} +1.00*BW +99.61$	8.5	0.5

Note: d_{C7-IJ} : C7 to IJ distance, $d_{T8-PSIS}$: Distance between T8 and PSIS midpoint, $d_{C7-PSIS}$: Distance between C7 and PSIS midpoint, d_{T8-PX} : T8 to PX distance, d_{C7-T8} : C7 to T8 distance,

137

138 **C7/T1 and L5/S1 prediction**

139 The regression equations to predict the vertical distance C7/T1 and L5/S1 from t_0 on S^{int} are listed in
 140 Table 3. Estimation of L5/S1 showed a higher error than C7/T1. $d_{C7/T1}$ and $d_{L5/S1}$ were defined at the
 141 intersection of $t_{C7/T1}$, respectively $t_{L5/S1}$, and S^{int} .

142 **Table 3. Predictors and regression coefficients to predict the spine extremities C7/T1 and L5/S1**
 143 **from spine shape descriptors and anthropometrics**

	Regression equations	RMSE (mm)	r^2
$t_{C7/T1}$	$- (-1.02*R + 0.07*Ch + 0.99)*R$	10.5	0.5
$t_{L5/S1}$	$- (0.49*CL_h + 0.92)*R$	18.3	0.4

Note: R, C_h and CL_h are described in Figure 3, height in mm, body weight (BW) in Kg. d_{C7-IJ} : C7 to IJ distance, d_{C7-T8} : C7 to T8 distance

144

145 **Mean curvilinear coordinates of the joint centers**

146 The relative positions (curvilinear abscises normalized by the curvature length) of the joint centers
 147 along the internal spinal profile were observed quite invariant among the subjects (SD < 5 mm, Table
 148 4).

149

150 **Table 4. Mean position of intervertebral joint centers along S^{int} normalized by the developed length**
 151 **of internal spline. Standard errors in percentage and in mm are indicated.**

	Mean	SD (%)	SD (mm)
C7/T1	0	0	0

T1/T2	4	0	1.57
T2/T3	9	1	2.4
T3/T4	13	1	3.11
T4/T5	18	1	3.13
T5/T6	23	1	3.54
T6/T7	28	1	3.94
T7/T8	33	1	4.23
T8/T9	38	1	4.52
T9/T10	43	1	4.83
T10/T11	49	1	4.75
T11/T12	55	1	4.76
T12/L1	61	1	4.69
L1/L2	69	1	4.68
L2/L3	76	1	4.68
L3/L4	84	1	4.46
L4/L5	92	0	2.99
L5/S1	100	0	1.82

152

153

154 **Evaluation**

155 2D distance between estimated and reference joint centers using both methods showed very similar
156 errors, respectively 9.7 mm (± 5.0) and 9.5 mm (± 5.0) with or without using the external back profile
157 (Table 5).

158

159 **Table 5.** Root mean square errors (RMSE) in x (antero-posterior), y (medio-lateral) and 2D distance
160 between reference and estimated joint centers using methods with or without using the external
161 back profiles (mm) on the training group of 80 subjects. Standard deviations are provided.

	Using the external back profile				Without using the external back profile			
	2D distance RMSE				2D distance RMSE			
	x	y	mean	SD	x	y	mean	SD
C7/T1	6.8	5.5	8.7	4.5	4.0	5.5	6.8	3.5
T1/T2	4.7	5.6	7.3	3.3	4.7	5.1	6.9	3.2
T2/T3	5.1	5.7	7.7	3.3	5.5	4.8	7.4	3.6
T3/T4	5.4	5.8	7.9	3.4	6.8	4.7	8.2	4.1
T4/T5	5.8	5.7	8.2	3.6	7.7	4.5	8.9	4.5
T5/T6	6.3	6.1	8.8	3.8	8.9	4.7	10.0	4.7
T6/T7	6.7	6.4	9.3	4.1	9.8	4.9	11.0	5.1
T7/T8	6.8	6.6	9.5	4.4	9.8	5.1	11.1	5.2

T8/T9	6.8	6.8	9.6	4.7	8.9	5.2	10.3	5.1
T9/T10	6.8	7.0	9.8	5.0	7.5	5.5	9.3	4.7
T10/T11	6.8	7.1	9.8	5.2	6.6	5.8	8.8	4.5
T11/T12	6.9	7.2	10.0	5.4	6.2	6.1	8.8	4.5
T12/L1	7.0	7.6	10.3	5.8	6.3	6.7	9.2	4.7
L1/L2	7.2	8.2	10.9	6.1	6.9	7.4	10.2	5.4
L2/L3	6.9	9.0	11.3	6.1	7.4	8.2	11.0	6.0
L3/L4	6.0	9.3	11.1	5.4	7.4	8.2	11.0	6.0
L4/L5	6.7	9.8	11.9	5.6	6.7	9.1	11.3	5.6
L5/S1	8.0	9.9	12.7	5.9	7.2	9.5	11.9	5.3
Total			9.7	5.5			9.5	5.0

Note: Equations showing larger RMS errors ($d_{0.4}^{int}$, $d_{0.7}^{int}$ and respectively $D_{0.3}$, $D_{0.7}$) were not used for the least square estimation of internal spine.

162

163 As the most precise regression equations were found with the method using the external back profile
 164 (Table 1), this method was applied for predicting joint centers location over the validation cohort of 13
 165 subjects. Mean error was 10.2 ± 5.6 mm (Table 6).

166

167 **Table 6. Mean error on 3D distance and standard error (SD) between estimated end reference joint**
 168 **centers on the validation group of additional 13 subjects (mm) using the back profile. A third**
 169 **orthogonal axis was added to the 2D local system and additional medio-lateral joint coordinates**
 170 **were supposed to be aligned with the t axis so that joint i was located with respectively (d,0,t)**
 171 **antero-posterior, medio-lateral and vertical coordinates.**

	Mean	SD
C7/T1	7.0	3.9
T1/T2	9.5	5.4
T2/T3	11.5	5.9
T3/T4	10.7	6.6
T4/T5	9.6	6.2
T5/T6	9.5	5.7
T6/T7	10.0	5.8
T7/T8	10.6	5.8
T8/T9	10.3	5.5
T9/T10	9.5	5.1
T10/T11	8.8	5.9
T11/T12	9.7	5.7
T12/L1	10.4	5.3

L1/L2	11.2	5.0
L2/L3	11.5	5.3
L3/L4	12.1	5.9
L4/L5	10.9	6.4
L5/S1	10.6	5.7
Total	10.2	5.6

172

173

174 Discussion

175 Two methods requiring a small amount of easily accessible inputs to predict all thoracic and lumbar
176 intervertebral joint centers location were compared. A focus was given on the sagittal plane where the
177 main variation in spine shape occur for asymptomatic subjects. Only small differences were obtained
178 between the methods either using only 6 ALS or using both 6 ALs and the external back profile.

179 Both methods were able to predict all the 18 thoracic and lumbar joint centers while most existing
180 geometrical models usually enabled to predict lumbar joint centers (Sicard *et al.* 1993, Lee *et al.* 1995,
181 Chiou *et al.* 1996) or a few joints, e.g. C2/C3, C7/T1, T4/T5, T8/T9, T12/L1, L2/L3 and L5/S1 (Snyder *et*
182 *al.* 1972). The mean error of 10.2 ± 5.6 mm was lower than the PCA-based method in Nérot *et al.* 2016
183 (12.8 ± 5.0 mm). This might be due to the pre-selection phase of candidate predictors at the areas with
184 thinner layers of soft tissues. Conversely the PCA method took into account the entire trunk surface
185 and associated shape variation, like in the belly region, which are probably independent to spine joints
186 location.

187 Extending Snyder *et al.*'s method for all joint centers was also considered. This alternative method
188 requires the estimation of 2 unknowns for each joint: the distance to its orthogonal projection on the
189 back profile and the curvilinear abscissa of this projection. But higher prediction errors may result from
190 higher number of unknowns. Moreover normal vectors to the back surface were hardly reproducible
191 depending on the quality of acquisition and the smoothing method. The advantages of the current
192 methods are to estimate a smaller number of unknown variables and to robustly define a unique
193 direction for calculating the spine coordinates in the sagittal plane.

194

195 L5/S1 estimated only using C7 and PSIS landmarks showed higher error compared to the PCA method
196 in Nérot *et al.* (2016) using the whole trunk surface including the pelvic region. This might highlight the
197 importance of considering some pelvic anatomical descriptors for L5/S1 prediction. For example, a
198 simple method for predicting the L5/S1 from pelvic landmarks was proposed in Peng *et al.* 2015. When

199 considering our methods while imposing the true position of L5/S1, errors on joint location were
200 reduced by 1 to 5 mm on average, confirming the importance of L5/S1 accurate prediction to precisely
201 locate the rest of the spine joints.

202 The major limitation of this method is that it is based on a standing posture and may not be applicable
203 to different posture involving different spinal curvatures (such as seating or supine). Furthermore, as
204 virtual palpation was performed, the influence of palpation errors on these regression methods needs
205 to be tested on a cohort of volunteers in future work.

206

207 **Conclusion**

208 This study proposed two geometric models allowing to predict spine joint centers from C7/T1 to L5/S1
209 with much less data than existing methods while improving the prediction precision. The methods are
210 adapted to current methodology in motion analysis and compliant with minimal lab equipment.
211 Prediction of L5/S1 using predictors from the pelvis could improve the results. Work is ongoing to
212 change the standing position to a desired posture such as seated one in order to enlarge the possibility
213 of applications.

214

215 **Acknowledgment**

216 The authors thank the ParisTech BiomecAM chair program on subject-specific musculoskeletal
217 modeling, and in particular COVEA and Société Générale, as well as IFSTTAR for the PhD grant.

218

219 **References**

220 Aubert B., Vergari C., Ilharreborde B., Courvoisier A., Skalli W. 3D reconstruction of rib cage geometry
221 from biplanar radiographs using a statistical parametric model approach. *Computer Methods in*
222 *Biomechanics*, 2014

223 Bryant J.T., Gavin J., Smith B.L., Stevenson J.M., Reid J.G., Smith B.L., Stevenson J.M. Method for
224 determining vertebral body positions in the sagittal plane using skin markers. *Spine*, 14(3):258-65,
225 1988

226 Chiou W.K., Lee Y.H., Chen W.J., Lee M., Lin Y.H. A non-invasive protocol for the determination of
227 lumbar spine mobility. *Clinical Biomechanics*, 11(8):474-480, 1996.

228 Choi H.Y., Kim K.M., Han J., Sah S., Kim S.H., Hwang S.H., Lee K.N., Pyun J.K., Montmayeur N., Marca

- 229 C., Haug E., Lee I. Human Body Modeling for Riding Comfort Simulation. In: Duffy V.G. (eds) Digital
230 Human Modeling. ICDHM 2007. Lecture Notes in Computer Science, vol 4561. Springer, Berlin,
231 Heidelberg
- 232 Drerup B. Rasterstereographic measurement of scoliotic deformity. *Scoliosis*, 9(1):22, 2014.
- 233 Dubousset J., Charpak G., Skalli W., Deguise J., Kalifa G. Eos : a New Imaging System With Low Dose
234 Radiation in Standing Position for Spine and Bone & Joint Disorders. *Journal of Musculoskeletal*
235 *Research*, 13(01):1-12, 2010.
- 236 Harlick J.C., Milosavljevic S., Milburn P.D. Palpation identification of spinous processes in the lumbar
237 spine. *Manual therapy*, 12(1):56-62, 2007
- 238 Himes J.H., Roche A.F., Siervogel R.M. Compressibility of skinfolds and the measurement of
239 subcutaneous fatness. *Am. J. Clin. Nutr.* 32:1734-1740, 1979
- 240 Humbert L., De Guise J. A., Aubert B., Godbout B., Skalli W. 3D reconstruction of the spine from biplanar
241 X-rays using parametric models based on transversal and longitudinal inferences. *Medical Engineering*
242 *& Physics*, 31(6):681_7, 2009.
- 243 Kennedy K.W. Workspace Evaluation and Design: USAF Drawing Board Manikins and the Development
244 of Cockpit Geometry Design Guides, *Anthropometry and Biomechanics: Theory and Application*,
245 Easterby, R.K., K.H.E. Kroemer and D.B. Chaffin (Eds.), Plenum Press, New York, USA, pp. 205-213, 1982.
- 246 Klipstein-Grobusch K., Georg T., Boeing H. Interviewer variability in anthropometric measurements and
247 estimates of body composition. *International Journal of Epidemiology*. 26 Suppl 1(1):S174-80, 1997
- 248 Lee Y.H., Chiou W.K., Chen W.J., Lee M.Y., Lin Y.H. Predictive model of intersegmental mobility of
249 lumbar spine in the sagittal plane from skin markers. *Clinical Biomechanics*, 10(8):413-420, 1995.
- 250 Lohmann T.G., Roche A.F., Martorell R. *Anthropometric Standardization Reference Manual*. Human
251 Kinetics. Champaign, IL. *Anthropometry in Body Composition An Overview J.*, 1988
- 252 Mitton D., Deschênes S., Laporte S., Godbout B., Bertrand S., de Guise J.A., Skalli W. 3D Reconstruction
253 of the pelvis from bi-planar radiography.pdf. *Computer Method in Biomechanics and Biomedical*
254 *Engineering*, 9(1):1_5, 2006.
- 255 Nérot A., Skalli W., Wang X. A principal component analysis of the relationship between the external
256 body shape and internal skeleton for the upper body. *J Biomech.* 3;49(14):3415-3422, 2016
- 257 Nérot A., Choisine J., Amabile C., Travert C., Pillet H., Wang X., Skalli W. A 3D reconstruction method of
258 the body envelope from biplanar X-rays : Evaluation of its accuracy and reliability. *Journal of*
259 *Biomechanics*, 48(16):4322_6, 2015.

- 260 Peng J., Panda J., Van Sint Jan S., Wang X. Methods for determining hip and lumbosacral joint centers
261 in a seated position from external anatomical landmarks. *Journal of Biomechanics*, 48(2):396-400,
262 2015.
- 263 Reed M.P., Manary M.A., Schneider L.W. Methods for measuring and representing automobile
264 occupant posture. *SAE International*, 108(724):1-14, 1999.
- 265 Sicard C., Gagnon M. A geometric model of the lumbar spine in the sagittal plane. *Spine*, 18(5):646-58,
266 1993.
- 267 Snyder R.G., Chaffin D.B., Schutz R.K. Link system of the human Torso. *Aerospace Medical Research*
268 *Laboratory, Wright-Patterson Air Force base, Ohio*.1972.n.p., 41(3):1974, 1972.
- 269 Steffen J.S., Obeid I., Aurouer N., Hauger O., Vital J.M., Dubousset J., Skalli W. 3D postural balance with
270 regard to gravity line : An evaluation in the transversal plane on 93 patients and 23 symptomatic
271 volunteers. *European Spine Journal*, 19(5):760-767, 2010.
- 272 Wang J., Thornton J.C., Kolesnik S., Pierson R.N. Anthropometry in body composition. An overview.
273 *Ann N Y Acad Sci*.904:317-26, 2000

<https://doi.org/10.1016/j.jbiomech.2017.11.013>
Journal of Biomechanics